Figure S1

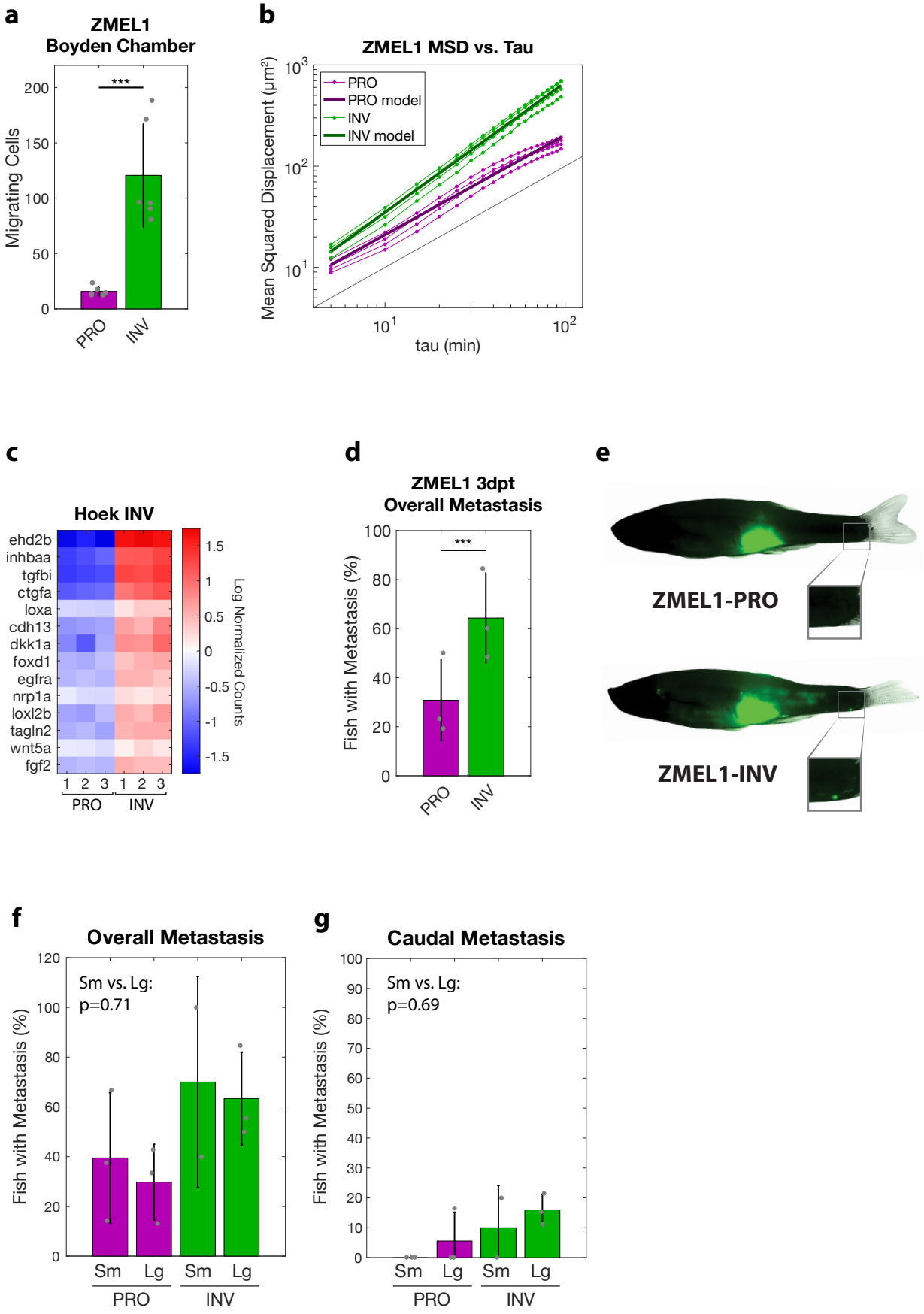
a
ZMEL1
Boyden Chamber
Migrating Cells
***
PRO
INV
b
ZMEL1 MSD vs. Tau
Mean Squared Displacement (μm²)
PRO
PRO model
INV
INV model
tau (min)
c
Hoek INV
ehd2b
inhbaa
tgfbi
ctgfa
loxa
cdh13
dkk1a
foxd1
egfra
nrp1a
loxl2b
tagln2
wnt5a
fgf2
Log Normalized Counts
PRO
INV
d
ZMEL1 3dpt
Overall Metastasis
Fish with Metastasis (%)
***
e
ZMEL1-PRO
ZMEL1-INV
f
Overall Metastasis
Sm vs. Lg:
p=0.71
Fish with Metastasis (%)
Sm
Lg
PRO
INV
g
Caudal Metastasis
Sm vs. Lg:
p=0.69
Fish with Metastasis (%)

Figure S1. PRO and INV coexist in zebrafish melanoma, with INV cells metastasizing more frequently due to increased extravasation (Related to Figure 1)

a. Number of ZMEL1 cells migrating in Boyden Chamber assay ($p<0.001$ by linear regression, N=3 independent experiments for each of 2 fluorophores). **b.** Log-log plot of mean squared displacement (MSD) vs. lag time (tau) over the range of $5 \leq tau < 100$ minutes with model fits overlaid (N=4 independent experiments, see Methods for details). The slope (α) provides quantification of the persistence of motility, where a cell moving randomly will have $\alpha=1$, and a cell moving along a straight line will have $\alpha=2$ (Gorelik and Gautreau, 2014). Black line with $\alpha=1$ is shown for comparison. **c.** Heatmap of genes in the Hoek INV signature that are differentially expressed in ZMEL1-INV vs. -PRO (log_2 fold change cutoff ± 1.5, $p_{adj}<0.05$). As in Figure 1e, but with zebrafish gene names. **d.** Quantification of overall distant metastases seeded by ZMEL1 populations at 3 dpt (OR [95% CI]: 4.49 [1.94, 10.43]; $p<0.001$ by logistic regression; N=3 independent experiments with PRO/INV 10/10, 31/33, and 13/13 fish per group, respectively; n=110 fish total; plot shows mean ± SD). **e.** Representative images of ZMEL1-PRO and -INV tumors and distant metastases (e.g. to caudal region [box]) at 3 days post-transplant (3dpt). **f-g.** Quantification of (f) overall metastasis and (g) caudal metastasis seeded by ZMEL1 populations at 3dpt stratified by primary tumor size (small vs. large). $p=0.71$ for overall metastasis and $p=0.69$ for caudal metastasis for comparison of small vs. large primary tumors by logistic regression; plot shows mean ± SD.

Figure S2

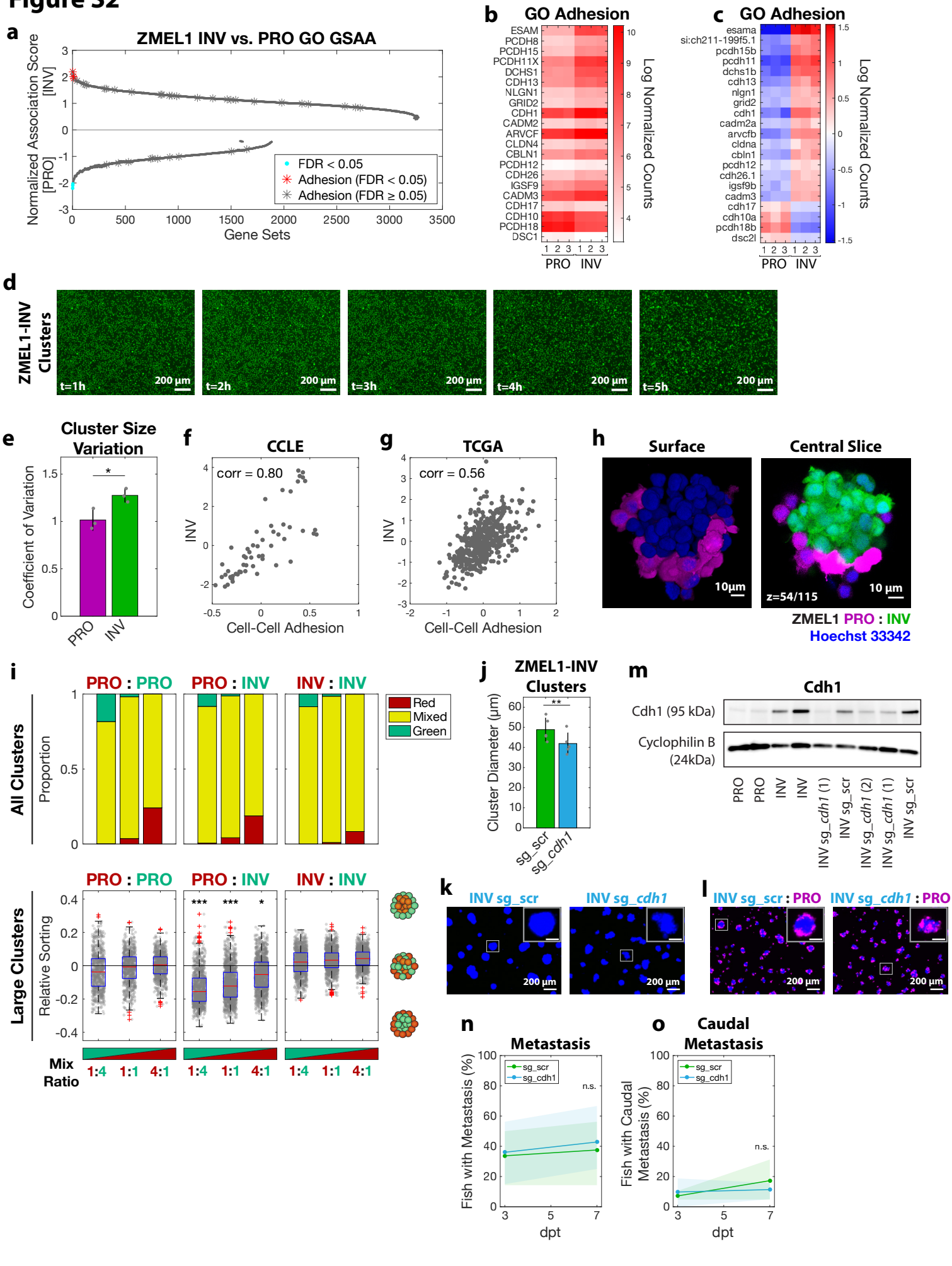
a
ZMEL1 INV vs. PRO GO GSAA
Normalized Association Score [INV]
Normalized Association Score [PRO]
Gene Sets
FDR < 0.05
Adhesion (FDR < 0.05)
Adhesion (FDR ≥ 0.05)
b
GO Adhesion
ESAM
PCDH8
PCDH15
PCDH11X
DCHS1
CDH13
NLGN1
GRID2
CDH1
CADM2
ARVCF
CLDN4
CBLN1
PCDH12
CDH26
IGSF9
CADM3
CDH17
CDH10
PCDH18
DSC1
Log Normalized Counts
PRO INV
c
GO Adhesion
esama
si:ch211-199f5.1
pcdh15b
pcdh11
dchs1b
cdh13
nlgn1
grid2
cdh1
cadm2a
arvcfb
cldna
cbln1
pcdh12
cdh26.1
igsf9b
cadm3
cdh17
cdh10a
pcdh18b
dsc2l
Log Normalized Counts
PRO INV
d
ZMEL1-INV Clusters
t=1h
t=2h
t=3h
t=4h
t=5h
200 μm
e
Cluster Size Variation
Coefficient of Variation
PRO
INV
f
CCLE
corr = 0.80
INV
Cell-Cell Adhesion
g
TCGA
corr = 0.56
INV
Cell-Cell Adhesion
h
Surface
Central Slice
10μm
z=54/115
10 μm
ZMEL1 PRO : INV
Hoechst 33342
i
All Clusters
Large Clusters
PRO : PRO
PRO : INV
INV : INV
Red
Mixed
Green
Proportion
Relative Sorting
Mix Ratio
1:4
1:1
4:1
j
ZMEL1-INV Clusters
Cluster Diameter (μm)
sg_scr
sg_cdh1
m
Cdh1
Cdh1 (95 kDa)
Cyclophilin B (24kDa)
PRO
PRO
INV
INV
INV sg_cdh1 (1)
INV sg_scr
INV sg_cdh1 (2)
INV sg_cdh1 (1)
INV sg_scr
k
INV sg_scr
INV sg_cdh1
200 μm
l
INV sg_scr : PRO
INV sg_cdh1 : PRO
200 μm
n
Metastasis
Fish with Metastasis (%)
sg_scr
sg_cdh1
n.s.
dpt
o
Caudal Metastasis
Fish with Caudal Metastasis (%)
sg_scr
sg_cdh1
n.s.
dpt

Figure S2. Cluster formation by INV state drives spatial patterning of melanoma clusters (Related to Figure 2)

a. Dual waterfall plot of all gene sets from GO analysis. Adhesion GO gene sets are indicated with an asterisk and colored according to false discovery rate (FDR). **b-c.** Heatmap of genes in adhesion GO gene sets (FDR < 0.05, n=3) that are differentially expressed between ZMEL1-PRO and -INV (log_2 fold change cutoff ± 1.5, $p_{adj} < 0.05$). As in Figure 2b, but with (b) absolute expression data, and (c) zebrafish gene names. **d.** Representative images of early stages of ZMEL1-INV cluster formation in Figure 2d. Times are calculated from initial plating of assay. **e.** Quantification of coefficient of variation (CV = σ/μ, where σ is the population standard deviation and μ the population mean) of cluster area of individual PRO and INV clusters at 2 days (p=0.026 by two-tailed t-test, N=3 independent experiments). **f-g.** Human melanoma samples from (f) The Cancer Cell Line Encyclopedia (CCLE, n=56) and (g) The Cancer Genome Atlas (TCGA) melanoma (SKCM, n=472) cohort are plotted as INV (Hoek et al., 2006) versus Cell-Cell Adhesion scores calculated from RNA-seq. Pearson correlation coefficient between scores is shown. **h.** (left) Composite 3D opacity rendering and (right) central slice of confocal imaging through co-cluster of ZMEL1-PRO and ZMEL1-INV. **i.** Quantification of (top) mixing and (bottom) sorting of heterotypic ZMEL1 clusters as in Figure 2f. Red (tdTomato) and green (EGFP) labeled ZMEL1 cells were mixed PRO:PRO, PRO:INV, and INV:INV at indicated ratios. (top) Quantification of all clusters revealed that nearly all clusters mix, regardless of cell type. (bottom) Spatial sorting was significantly enriched in PRO:INV clusters compared to PRO:PRO and INV:INV controls ($p<0.001$, $p<0.001$, and $p=0.038$ for 1:4, 1:1, and 4:1, respectively, by one-way ANOVA on mean of each replicate versus respective PRO:PRO and INV:INV controls [greater of two p-values reported]). **j.** Cluster size after 2 days in ZMEL1-INV with CRISPR deletion of *cdh1* (sg_*cdh1*)

versus control (sg_scr) (p=0.0016, two-tailed paired t-test, N=5 independent experiments). **k.** Representative images of effect of sg_*cdh1* versus sg_scr on cluster size at 3 days (inset scale 50 μm). **l.** Representative composite images of mixing effects of sg_*cdh1* versus sg_scr. Control (sg_scr) ZMEL1-INV cells mixed with ZMEL1-PRO show clear spatial sorting, whereas sg_*cdh1* ZMEL1-INV cells mixed with ZMEL1-PRO demonstrate decreased sorting (inset scale 50 μm). **m.** Western blot confirmed two different sg_*cdh1*'s decreased Cdh1 protein expression in ZMEL1-INV to a level comparable to ZMEL1-PRO. sg_*cdh1* (1) was utilized for all phenotypic experiments. **n-o.** ZMEL1-INV orthotopic primary tumors with sg_*cdh1* do not seed (n) distant metastases and (o) caudal metastases in a significantly different percentage of zebrafish than with sg_scr control (p=0.56 and p=0.44, respectively, at 7 dpt by logistic regression; N=3 independent experiments with sg_scr/sg_cdh1 16/15, 21/20, 19/19 fish per group, respectively; n=110 fish total).

Figure S3

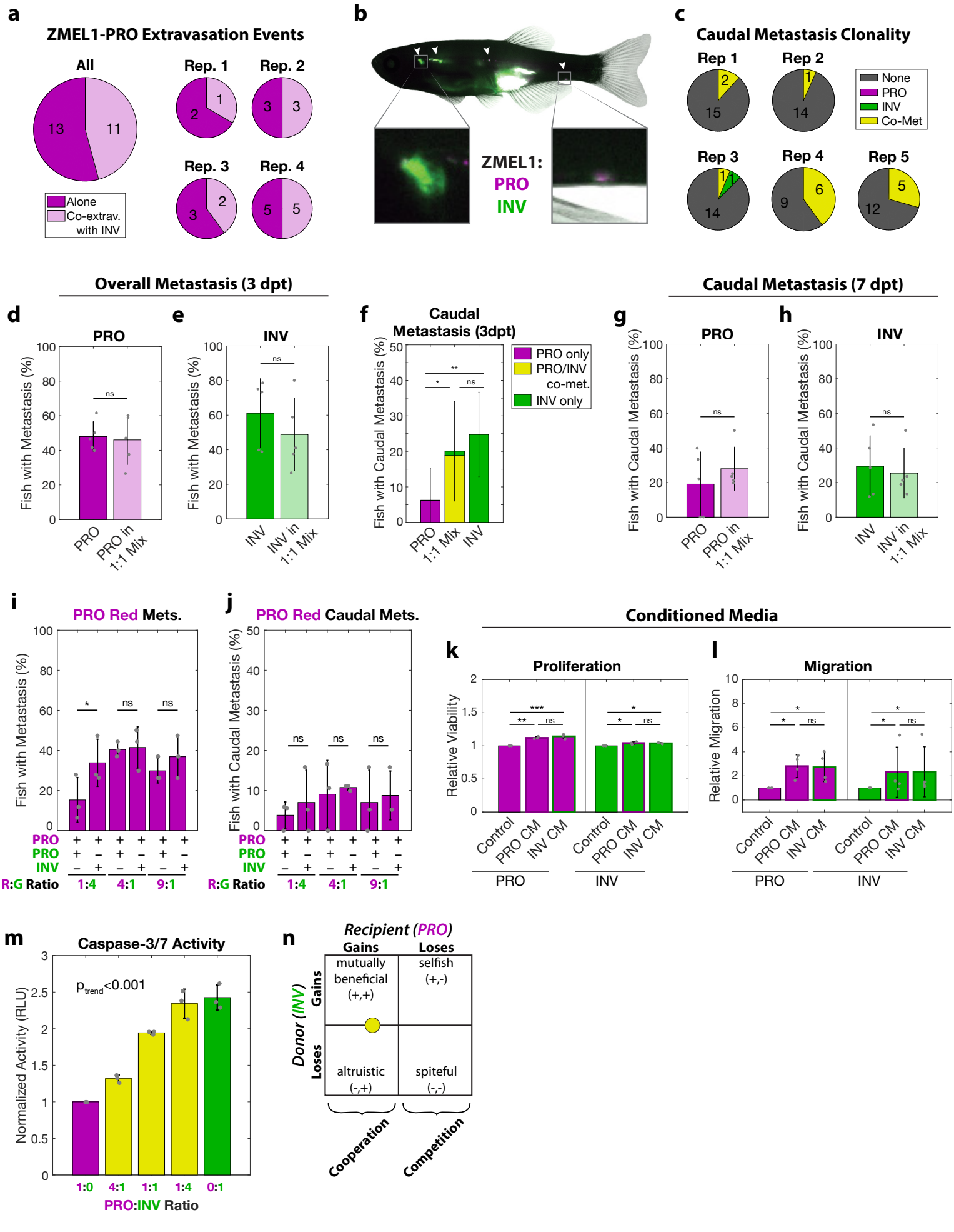
a
ZMEL1-PRO Extravasation Events
All
13
11
Alone
Co-extrav. with INV
Rep. 1
2
1
Rep. 2
3
3
Rep. 3
3
2
Rep. 4
5
5
b
ZMEL1:
PRO
INV
c
Caudal Metastasis Clonality
Rep 1
2
15
Rep 2
1
14
None
PRO
INV
Co-Met
Rep 3
1
1
14
Rep 4
6
9
Rep 5
5
12
Overall Metastasis (3 dpt)
Caudal Metastasis (7 dpt)
d
PRO
Fish with Metastasis (%)
ns
PRO
PRO in 1:1 Mix
e
INV
Fish with Metastasis (%)
ns
INV
INV in 1:1 Mix
f
Caudal Metastasis (3dpt)
Fish with Caudal Metastasis (%)
**
*
ns
PRO only
PRO/INV co-met.
INV only
PRO
1:1 Mix
INV
g
PRO
Fish with Caudal Metastasis (%)
ns
PRO
PRO in 1:1 Mix
h
INV
Fish with Caudal Metastasis (%)
ns
INV
INV in 1:1 Mix
i
PRO Red Mets.
Fish with Metastasis (%)
*
ns
ns
PRO + + + + + +
PRO + − + − + −
INV − + − + − +
R:G Ratio 1:4 4:1 9:1
j
PRO Red Caudal Mets.
Fish with Caudal Metastasis (%)
ns
ns
ns
PRO + + + + + +
PRO + − + − + −
INV − + − + − +
R:G Ratio 1:4 4:1 9:1
Conditioned Media
k
Proliferation
Relative Viability
***
**
ns
*
*
ns
Control
PRO CM
INV CM
Control
PRO CM
INV CM
PRO
INV
l
Migration
Relative Migration
*
*
ns
*
*
ns
Control
PRO CM
INV CM
Control
PRO CM
INV CM
PRO
INV
m
Caspase-3/7 Activity
Normalized Activity (RLU)
p trend <0.001
1:0 4:1 1:1 1:4 0:1
PRO:INV Ratio
n
Recipient (PRO)
Gains
Loses
Donor (INV)
Gains
Loses
mutually beneficial (+,+)
selfish (+,-)
altruistic (-,+)
spiteful (-,-)
Cooperation
Competition

Figure S3. PRO and INV cooperate in metastasis via co-extravasation (Related to Figure 3)

a. Number of observed extravasation events of ZMEL1-PRO either alone or in the form of co-extravasation with ZMEL1-INV following intravenous transplant (p=0.18 by two-tailed paired t-test, N=4 independent experiments with 14, 15, 22, and 22 fish each; n=73 fish total). **b.** Composite image of adult zebrafish with orthotopic transplants of 1:1 mixtures of ZMEL1-PRO and -INV seed polyclonal metastases (arrowheads), including to the kidney and caudal regions (left and right boxes, respectively). **c.** Number of fish co-transplanted with a 1:1 mixture of ZMEL1-PRO and -INV that have no caudal metastases (None), caudal metastases comprised of exclusively PRO or INV, or caudal metastases formed by co-metastasis (Co-Met) of both cell types (N=5 independent experiments with 17, 15, 16, 15, and 17 fish each; 80 fish total; $p<0.001$ by Mantel-Haenszel's test for null hypothesis of no interaction; as in Figure 3c for each independent experiment). **d.** ZMEL1-PRO and **e.** ZMEL1-INV showed similar levels of overall metastasis at 3 dpt in mixed tumors compared to when each was transplanted alone (p=0.83 and p=0.13, respectively, by logistic regression). **f.** Proportion of fish with caudal ZMEL1-PRO only, ZMEL1-INV only, or PRO/INV co-metastasis (co-met) at 3dpt (PRO vs. INV: p=0.0054; "PRO only" in PRO vs. 1:1 mix: p=0.033; "INV only" in INV vs. 1:1 mix: p=0.49; all by logistic regression). Alternate presentation of data in Figure 3d-e. **g-h.** (g) ZMEL1-PRO and (h) ZMEL1-INV showed similar levels of caudal metastasis at 7 dpt in mixed tumors compared to when each was transplanted alone (p=0.54 and p=0.63, respectively, by logistic regression). For **b-h**: N=5 independent experiments with PRO/MIX/INV 18/17/18, 13/15/14, 15/16/15, 12/15/15, and 15/17/16 fish per group, respectively; 231 fish total; plots show mean ± SD). **i-j.** Adult zebrafish were orthotopically transplanted with an equivalent final concentration of tdTomato-labeled ZMEL1-PRO mixed at a 1:4, 4:1, or 9:1 ratio with EGFP-labeled ZMEL1-PRO or ZMEL1-INV. tdTomato-labeled ZMEL1-PRO (i)

overall metastases and (j) caudal metastases were quantified 3dpt to measure the impact of cooperation with ZMEL1-INV. ZMEL1-PRO metastasized more when co-transplanted with ZMEL1-INV than with ZMEL1-PRO in Red:Green 1:4 transplants (OR [95% CI]: 2.78 [1.09, 7.10]; p=0.032 by logistic regression). A total of N=3 independent variable ratio mixing experiments were performed, each with at least 16 fish per group (n=108/113/113 fish per replicate; n=334 fish total). **k-l.** Proliferation (k) and Boyden chamber migration (l) were quantified in ZMEL1-PRO and -INV cells with or without conditioned media (CM) from ZMEL1-PRO and -INV cells (p-values by linear regression; N=3 independent experiments for proliferation; N=4 independent experiments for migration). **m.** Caspase-3/7 activity normalized to cell number for clusters of indicated ratio of ZMEL1-PRO and -INV cells at 2 days. P-value for trend of normalized caspase-3/7 activity with increasing INV composition by linear regression (adjusted R-squared 0.91). **n.** The interaction between INV (donor) and PRO (recipient) cells can be schematically represented as a donor-recipient interaction (Hauser et al., 2009) falling into a regime of cooperation.

Figure S4

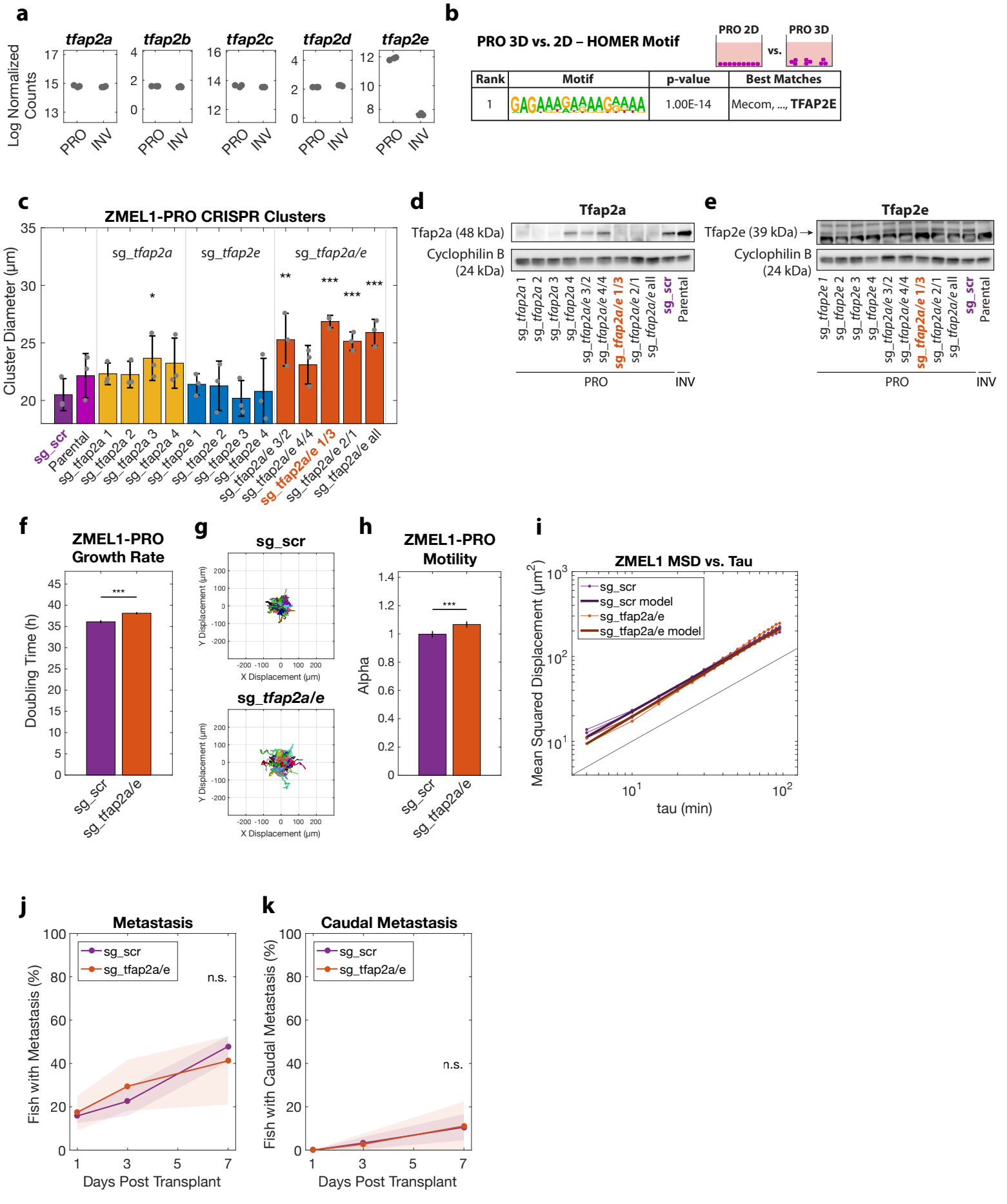
a
tfap2a
tfap2b
tfap2c
tfap2d
tfap2e
Log Normalized Counts
PRO
INV
b
PRO 3D vs. 2D – HOMER Motif
PRO 2D
vs.
PRO 3D
Rank
Motif
p-value
Best Matches
1
1.00E-14
Mecom, ..., TFAP2E
c
ZMEL1-PRO CRISPR Clusters
Cluster Diameter (µm)
sg_tfap2a
sg_tfap2e
sg_tfap2a/e
sg_scr
Parental
sg_tfap2a 1
sg_tfap2a 2
sg_tfap2a 3
sg_tfap2a 4
sg_tfap2e 1
sg_tfap2e 2
sg_tfap2e 3
sg_tfap2e 4
sg_tfap2a/e 3/2
sg_tfap2a/e 4/4
sg_tfap2a/e 1/3
sg_tfap2a/e 2/1
sg_tfap2a/e all
d
Tfap2a
Tfap2a (48 kDa)
Cyclophilin B (24 kDa)
PRO
INV
e
Tfap2e
Tfap2e (39 kDa)
Cyclophilin B (24 kDa)
PRO
INV
f
ZMEL1-PRO Growth Rate
Doubling Time (h)
sg_scr
sg_tfap2a/e
g
sg_scr
sg_tfap2a/e
Y Displacement (µm)
X Displacement (µm)
h
ZMEL1-PRO Motility
Alpha
sg_scr
sg_tfap2a/e
i
ZMEL1 MSD vs. Tau
Mean Squared Displacement (µm²)
tau (min)
sg_scr
sg_scr model
sg_tfap2a/e
sg_tfap2a/e model
j
Metastasis
Fish with Metastasis (%)
Days Post Transplant
sg_scr
sg_tfap2a/e
n.s.
k
Caudal Metastasis
Fish with Caudal Metastasis (%)
Days Post Transplant
sg_scr
sg_tfap2a/e
n.s.

Figure S4. TFAP2 distinguishes PRO vs. INV state and modulates clustering and metastasis (Related to Figure 4)

a. Boxplots of *tfap2a-e* expression from RNA-seq of ZMEL1-PRO and -INV. **b.** HOMER de-novo motif analysis of genes differentially expressed between ZMEL1-PRO in 3D (clusters) vs. 2D (no clusters) (log_2 fold change cutoff ± 1.5, $p_{adj} < 0.05$, ±500bp of transcription start site [TSS]). **c.** Cluster size in ZMEL1-PRO with CRISPR-Cas9 inactivation of *tfap2a* or *tfap2e* alone and in combination (p-values by linear regression; N=3 independent experiments). sgRNAs highlighted in purple (sg_scr) and orange (sg_*tfap2a/e* 1/3) were used for further experiments (Figures 4,5 and Figures S4,S5). **d-e.** Western blot confirmation of CRISPR inactivation of (d) *tfap2a* and (e) *tfap2e* with each sgRNA or combination of sgRNAs. **f-i.** Tracking of individual cells by time-lapse microscopy (N=3 independent experiments). **f.** ZMEL1-PRO with sg_*tfap2a/e* has slowed growth versus sg_scr ($p<0.001$ by linear regression, model estimates ± 95% CI shown). **g.** Representative displacements of 500 tracks per sgRNA. **h.** Model estimates ± 95% CI for alpha, the slope of the log-log plot of mean squared displacement vs. lag time (tau) for each ZMEL1-PRO sg_*tfap2a/e* and sg_scr ($p<0.001$ by linear regression). Larger alpha indicates more persistent motion. **i.** Log-log plot of mean squared displacement (MSD) vs. lag time (tau) over the range of $5 \leq tau < 100$ minutes with model fits overlaid (see Methods for details). The slope (α) provides quantification of the persistence of motility, where a cell moving randomly will have α=1, and a cell moving along a straight line will have α=2 (Gorelik and Gautreau, 2014). Black line with α=1 is shown for comparison. **j-k.** ZMEL1-PRO orthotopic primary tumors with sg_*tfap2a/e* do not seed (j) distant metastases and (k) caudal metastases in a significantly different proportion of zebrafish than with sg_scr control (p=0.44 and p=0.90, respectively, at 7 dpt by logistic regression; N=3 independent

experiments with sg_scr/sg_tfap2a/e 24/22, 22/22, 24/24 fish per group, respectively; n=138 fish total).

Figure S5

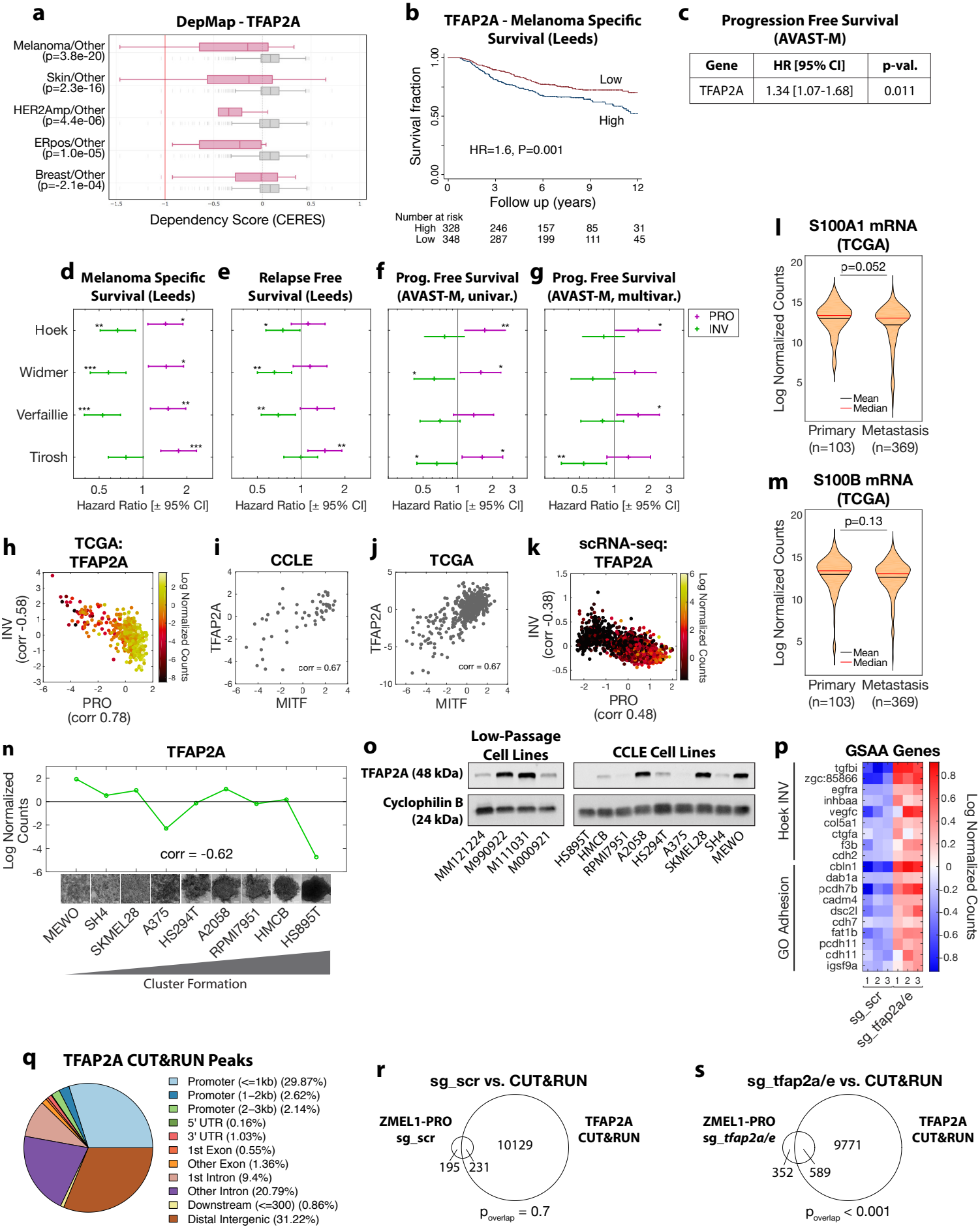
a
DepMap - TFAP2A
Melanoma/Other (p=3.8e-20)
Skin/Other (p=2.3e-16)
HER2Amp/Other (p=4.4e-06)
ERpos/Other (p=1.0e-05)
Breast/Other (p=-2.1e-04)
Dependency Score (CERES)
b
TFAP2A - Melanoma Specific Survival (Leeds)
Survival fraction
Low
High
HR=1.6, P=0.001
Follow up (years)
Number at risk
High 328 246 157 85 31
Low 348 287 199 111 45
c
Progression Free Survival (AVAST-M)
Gene | HR [95% CI] | p-val.
TFAP2A | 1.34 [1.07-1.68] | 0.011
d
Melanoma Specific Survival (Leeds)
e
Relase Free Survival (Leeds)
f
Prog. Free Survival (AVAST-M, univar.)
g
Prog. Free Survival (AVAST-M, multivar.)
PRO
INV
Hoek
Widmer
Verfaillie
Tirosh
Hazard Ratio [± 95% CI]
l
S100A1 mRNA (TCGA)
p=0.052
Log Normalized Counts
Mean
Median
Primary (n=103)
Metastasis (n=369)
m
S100B mRNA (TCGA)
p=0.13
h
TCGA: TFAP2A
INV (corr -0.58)
PRO (corr 0.78)
Log Normalized Counts
i
CCLE
TFAP2A
MITF
corr = 0.67
j
TCGA
k
scRNA-seq: TFAP2A
INV (corr -0.38)
PRO (corr 0.48)
n
TFAP2A
Log Normalized Counts
corr = -0.62
MEWO
SH4
SKMEL28
A375
HS294T
A2058
RPMI7951
HMCB
HS895T
Cluster Formation
o
Low-Passage Cell Lines
CCLE Cell Lines
TFAP2A (48 kDa)
Cyclophilin B (24 kDa)
MM121224
M990922
M111031
M000921
HS895T
HMCB
RPMI7951
A2058
HS294T
A375
SKMEL28
SH4
MEWO
p
GSAA Genes
Hoek INV
GO Adhesion
tgfbi
zgc:85866
egfra
inhbaa
vegfc
col5a1
ctgfa
f3b
cdh2
cbln1
dab1a
pcdh7b
cadm4
dsc2l
cdh7
fat1b
pcdh11
cdh11
igsf9a
Log Normalized Counts
sg_scr
sg_tfap2a/e
q
TFAP2A CUT&RUN Peaks
Promoter (<=1kb) (29.87%)
Promoter (1–2kb) (2.62%)
Promoter (2–3kb) (2.14%)
5' UTR (0.16%)
3' UTR (1.03%)
1st Exon (0.55%)
Other Exon (1.36%)
1st Intron (9.4%)
Other Intron (20.79%)
Downstream (<=300) (0.86%)
Distal Intergenic (31.22%)
r
sg_scr vs. CUT&RUN
ZMEL1-PRO sg_scr
TFAP2A CUT&RUN
10129
195
231
p_overlap = 0.7
s
sg_tfap2a/e vs. CUT&RUN
ZMEL1-PRO sg_tfap2a/e
TFAP2A CUT&RUN
9771
352
589
p_overlap < 0.001

Figure S5. TFAP2 correlates with clustering in human melanoma and regulates genes associated with metastasis and cell-cell adhesion (Related to Figure 5)

a. Analysis of TFAP2A in the Dependency Map (DepMap, CRISPR (Avana) Public 19Q3) dataset reveals a dependence of melanoma proliferation on TFAP2A. **b-c.** High TFAP2A mRNA expression in primary tumors predicts worse (b) melanoma specific survival in patients in the Leeds Melanoma Cohort (HR [95% CI]: 1.6 [1.2, 2.1], p=0.001 upper vs. lower half by Cox proportional hazards and (c) progression free survival in patients in the AVAST-M Melanoma Cohort (multivariate Cox regression model). **d-g.** Primary tumors with high PRO or low INV expression are associated with worse outcomes in patients in (d-e) the Leeds Melanoma Cohort and (f-g) the AVAST-M Melanoma Cohort. **h.** Human melanoma samples from The Cancer Genome Atlas (TCGA) melanoma (SKCM, n=472) cohort are plotted as PRO and INV scores (Hoek et al., 2006) calculated from RNA-seq and colored according to TFAP2A mRNA expression. Pearson correlation coefficients between TFAP2A and PRO/INV scores are shown on axes. **i-j.** Expression of TFAP2A and MITF in human melanoma samples from (i) CCLE (n=56) and (j) TCGA melanoma (SKCM, n=472) cohort are plotted with Pearson correlation coefficient. **k.** Individual human melanoma cells are plotted as PRO and INV scores (Hoek et al., 2006) calculated from single-cell RNA-seq and colored according to TFAP2A mRNA expression (re-analyzed from Jerby-Arnon et al. (Jerby-Arnon et al., 2018)). Pearson correlation coefficients between TFAP2A and PRO/INV scores are shown on axes. **l-m.** (l) S100A1 and (m) S100B mRNA expression in The Cancer Genome Atlas (TCGA) melanoma (SKCM) cohort comparing primary tumors and metastases (p-values by Wilcoxon rank sum test with Bonferroni correction). **n.** Human melanoma cell lines ranked by cluster forming ability (left to right: low to high) demonstrate negative correlation between TFAP2A mRNA expression by RNA-seq and clustering

(Spearman correlation shown). **o.** Western blot analysis of TFAP2A expression in panels of (left) low-passage human melanoma cell lines and (right) human melanoma cell lines. **p.** Heatmap of top genes in Hoek INV and GO Adhesion gene sets that are differentially expressed between ZMEL1-PRO sg_*tfap2a/e* and sg_scr (log_2 fold change cutoff ± 0.5, $p_{adj} < 0.05$). As in Figure 5f, but with zebrafish gene names. **q.** Distribution of TFAP2A CUT&RUN peaks as annotated by ChIPSeeker. **r-s.** Overlap of TFAP2A CUT&RUN peaks with genes upregulated in ZMEL1-PRO following CRISPR/Cas9 with (r) sg_scr ($p=0.7$ by bootstrapping) and (s) sg_*tfap2a/e* ($p<0.001$ by bootstrapping).

Figure S6

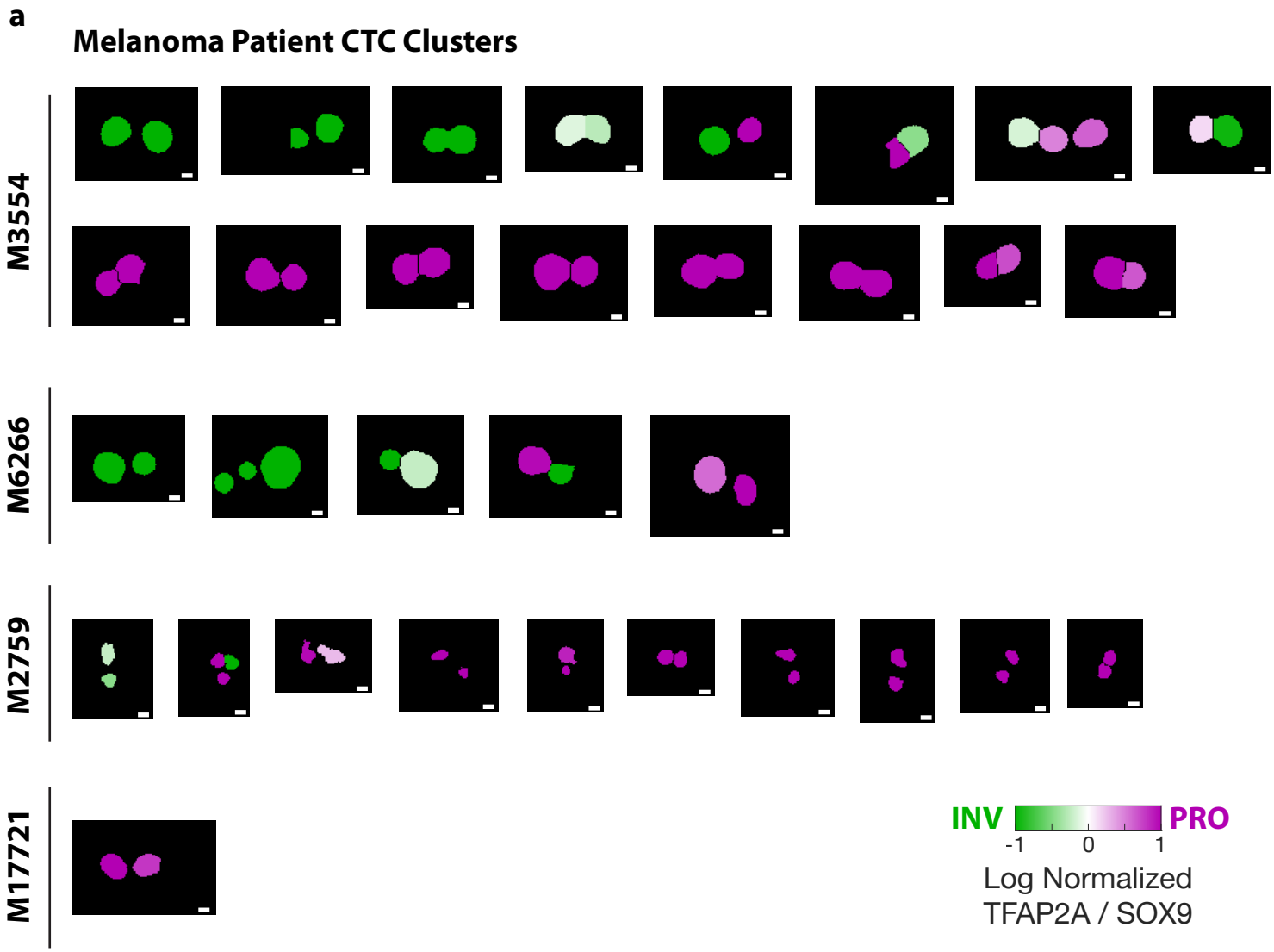
a
Melanoma Patient CTC Clusters
M3554
M6266
M2759
M17721
INV
PRO
-1
0
1
Log Normalized
TFAP2A / SOX9

Figure S6. PRO-INV heterotypic CTC clusters exist in the blood of melanoma patients (Related to Figure 6)

a. Nuclear quantification of TFAP2A and SOX9 in melanoma CTC clusters. n=32 clusters from four patients. Five additional patients were analyzed with no CTC clusters identified. Clusters were defined as two or more $TFAP2A^{pos}$; $CD45^{neg}$ cells. DAPI staining was used to generate nuclear masks for quantification. Scale bar is 5μm.

Figure S7

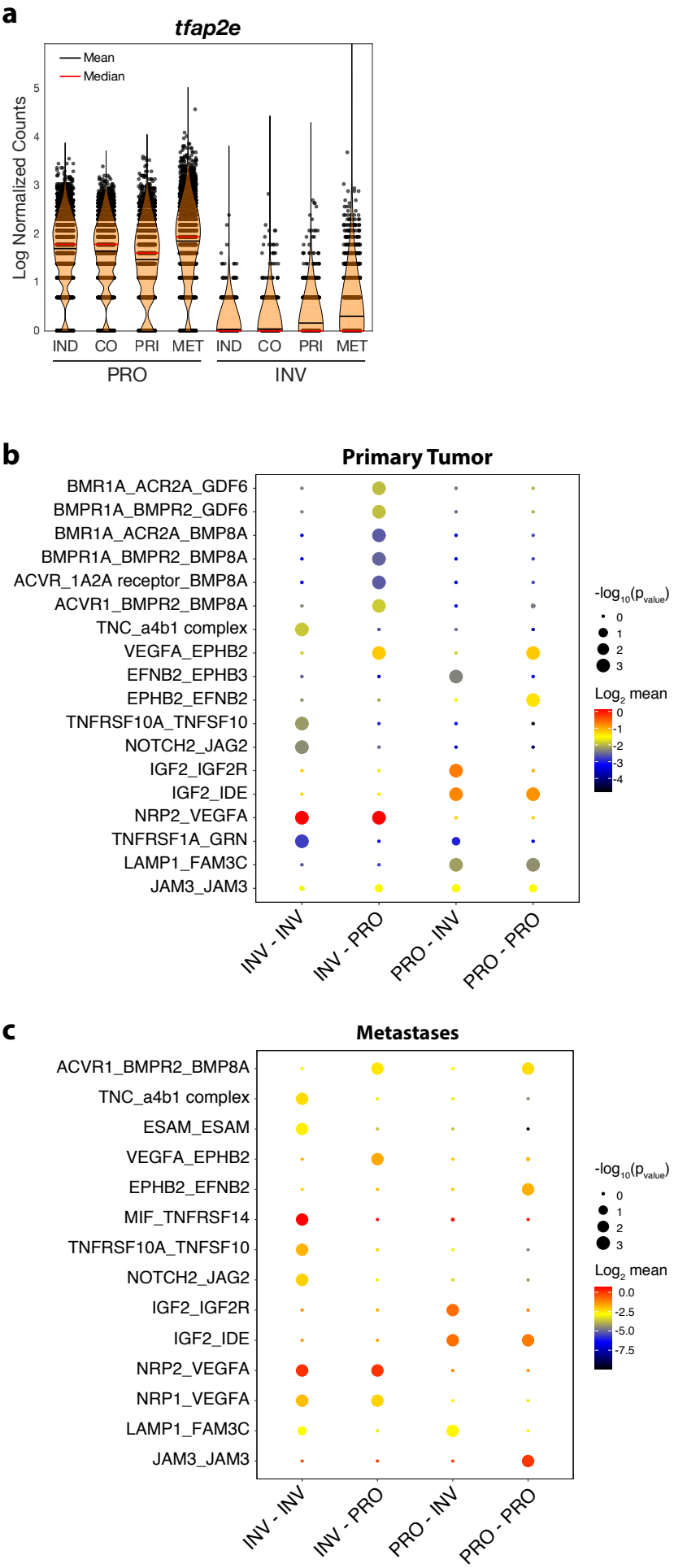
a
tfap2e
Mean
Median
Log Normalized Counts
0
1
2
3
4
5
IND
CO
PRI
MET
IND
CO
PRI
MET
PRO
INV
b
Primary Tumor
BMR1A_ACR2A_GDF6
BMPR1A_BMPR2_GDF6
BMR1A_ACR2A_BMP8A
BMPR1A_BMPR2_BMP8A
ACVR_1A2A receptor_BMP8A
ACVR1_BMPR2_BMP8A
TNC_a4b1 complex
VEGFA_EPHB2
EFNB2_EPHB3
EPHB2_EFNB2
TNFRSF10A_TNFSF10
NOTCH2_JAG2
IGF2_IGF2R
IGF2_IDE
NRP2_VEGFA
TNFRSF1A_GRN
LAMP1_FAM3C
JAM3_JAM3
INV - INV
INV - PRO
PRO - INV
PRO - PRO
-log10(pvalue)
0
1
2
3
Log2 mean
0
-1
-2
-3
-4
c
Metastases
ACVR1_BMPR2_BMP8A
TNC_a4b1 complex
ESAM_ESAM
VEGFA_EPHB2
EPHB2_EFNB2
MIF_TNFRSF14
TNFRSF10A_TNFSF10
NOTCH2_JAG2
IGF2_IGF2R
IGF2_IDE
NRP2_VEGFA
NRP1_VEGFA
LAMP1_FAM3C
JAM3_JAM3
INV - INV
INV - PRO
PRO - INV
PRO - PRO
-log10(pvalue)
0
1
2
3
Log2 mean
0.0
-2.5
-5.0
-7.5

Figure S7. Longitudinal single-cell RNA-seq reveals stability of PRO but not INV state (Related to Figure 7)

a. Single-cell expression of *tfap2e* in ZMEL1-PRO and -INV cells. Individual culture (IND); co-culture (CO); primary tumors (PRI); metastases (MET). **b-c.** CellPhoneDB results indicating ligand-receptor pairs that are significantly enriched for the indicated cell-cell interactions in (b) primary tumors and (c) metastases comprised of both ZMEL1-PRO and -INV. Ligand-receptor pairings are listed in order of cell pairings on x-axis.

Table S7. Melanoma patient CTC cluster statistics (Related to Figure 6)

Patient ID	Age Range	Sex	Mutation Status	Months from sampling to death	Total number of clusters isolated	Number of PRO clusters	Number of PRO-INV clusters	Number of INV clusters
M3554	61-65	F	$BRAF^{L597Q}$	1	16	8	4	4
M6266	61-65	M	$NRAS^{Q61K}$	0	5	1	1	3
M2759	61-65	F	$GNAQ^{Q209L}$	2	10	8	1	1
M17721	81-85	M	BRAF WT, NRAS WT	3	1	1	0	0
M2290	66-70	M	NRAS mutation in exon 3	1	0	n/a	n/a	n/a
M6590	76-80	M	$BRAF^{G466E}$	1	0	n/a	n/a	n/a
M9799	56-60	M	$NRAS^{Q61K}$	6	0	n/a	n/a	n/a
M7579	66-70	M	$BRAF^{V600K}$	1	0	n/a	n/a	n/a
M10803	81-85	M	BRAF WT, NRAS WT	2	0	n/a	n/a	n/a